Multiphonon effects in the one-phonon cross section of Al

R. Zivieri, G. Santoro, and V. Bortolani
Dipartimento di Fisica and INFM Unità di Ricerca di Modena, Università degli Studi di Modena, Via Campi 213/A, I-41100 Modena, Italy
(Received 24 February 1998)

We present a theoretical analysis of the phonon linewidth and energy shift observed with neutron spectroscopy in the one-phonon resonances. To take full account of the anharmonicity of the crystal we use a molecular-dynamics approach to evaluate the atomic displacement-displacement correlation functions. The atoms in the crystal interact with a semiempirical many-body potential and anharmonic effects of all orders are taken into account. The linewidths are evaluated for Al at two different temperatures, 80 and 300 K, in the high-symmetry directions of the crystal. Our results reproduce well the experimental data. The larger damping of the longitudinal phonons compared to that one of transverse phonons is fully explained in terms of anharmonic effects. Our analysis also confirms the anomalous behavior of the energy shift for longitudinal phonons in the [111] direction. [S0163-1829(98)09933-0]

I. INTRODUCTION

The inelastic scattering of neutrons by a crystal has proved to be a powerful tool to investigate the anharmonic properties of solids.[1,2] The effects of lattice anharmonicity are particularly evident in the one-phonon peak in the neutron-scattering cross section. In the harmonic approximation the one-phonon peak is a delta function centered at the frequency of the emitted or absorbed phonon from which neutrons are scattered. In an anharmonic crystal this delta function is broadened and shifted in position. For this reason many of the theoretical investigations were addressed in the study of the one-phonon peak broadening and energy shift. The theories of these phenomena were worked out in the 1960s by Van Hove,[3] Glauber,[4] Kokkedee,[5] and Maradudin and Fein[1] who presented detailed expressions for cubic and quartic anharmonicity.

In this paper we present a molecular-dynamics (MD) study of the displacement-displacement correlation functions that appear in the cross section. The molecular dynamics approach fully takes into account the anharmonic nature of the interatomic potential in the determination of the correlation functions. We have chosen to study the linewidths of Al since precise measurements[6,7] are available.

To perform the computer simulation of the correlation function, which involves thousands of atoms and a long simulation time of the order of nanoseconds, we use a classical interatomic potential. *Ab initio* calculations are not yet suitable for long-time simulations. For this reason we will use a many-body potential with parameters determined by first-principle calculations to describe properly the forces among atoms in a distorted crystal. This potential is briefly discussed in Sec. II. The molecular dynamics method used in the calculations is presented in Sec. III. The correlation functions we will use are described in Sec. IV. The results of our analysis both for longitudinal and transverse phonons in the high-symmetry directions are presented and discussed in Sec. V. The conclusions are drawn in Sec. VI.

II. MANY-BODY POTENTIAL

In order to perform the molecular dynamics simulation we use a many-body potential constructed according to the embedding-atom method[8,9] defined by the form

$$V=\frac{1}{2}\sum_{i,j\neq i}\phi(R_{ij})+\sum_{i}U(\rho_i) \tag{1}$$

with $\rho_i=\Sigma_{j\neq i}\rho(R_{ij})$. The first term represents a central potential between the atom in the actual position $\mathbf{R}_i$ and the atom in $\mathbf{R}_j$ with $R_{ij}=|\mathbf{R}_i-\mathbf{R}_j|$; the second term is the glue term,[10] where U represents a nonlinear function of ρ while ρ_i is a fictitious atomic charge on atom $\mathbf{R}_i$ that takes into account the neighboring sites. The functions ϕ, ρ, and U are determined by fitting the total potential to *ab initio* calculations of the forces in many atomic configurations.[8] In particular U violates the Cauchy relations among the elastic constants of the crystal and it describes accurately the forces acting on the atoms out of the equilibrium position. The range of the interactions extends up to 5.56 Å and after this distance the potential is set to zero.[8] With the potential of Eq. (1) we can perform long-time simulations with an accuracy comparable to that of the *ab initio* calculations.

III. MOLECULAR-DYNAMICS SIMULATION

The classical equations of motion can be written as

$$\frac{d^2}{dt^2}\mathbf{R}_i=-\frac{1}{m}\sum_{j(\neq i)}\bar{\alpha}_{ij}\mathbf{R}_{ij}, \tag{2}$$

where

$$\bar{\alpha}_{ij}=\alpha_{ij}+\left(\frac{\partial U_i}{\partial\rho_i}+\frac{\partial U_j}{\partial\rho_j}\right)\lambda_{ij}, \tag{3}$$

with

$$\alpha_{ij}=\frac{1}{R_{ij}}\frac{\partial\phi}{\partial R_{ij}}, \tag{4}$$

and

$$\lambda_{ij}=\frac{1}{R_{ij}}\frac{\partial\rho_{ij}(R_{ij})}{\partial R_{ij}}. \tag{5}$$

To integrate the equations of motion we have used the Gear predictor-corrector algorithm,[11,12] obtaining the instantaneous positions $\mathbf{R}_i(t)$ for each time step. To simulate the bulk of Al we have chosen a cubic supercell on which we impose periodic boundary conditions.[13] To obtain convergent results, as discussed later on, we take the number of atoms N in the supercell to range between 500–4000 atoms.

Our molecular dynamics simulation code fully takes into account the anharmonic nature of the interatomic potential in the evaluation of the correlation functions. It proceeds by the following steps. We start by taking zero kinetic energy and we randomize the positions of the N particles in order to have net forces among particles. Then we introduce the kinetic energy term and we solve the equations of motion. After 200–1000 step intervals the system reaches an equilibrium configuration. We allow the volume to expand uniformly. We then fix the temperature of interest. The system reaches this temperature after a few thousand time steps. At this point we fix the volume at that given temperature and we perform again 1000–2000 time steps without imposing any constraint on the kinetic energy. The system reaches an equilibrium configuration and the total energy remains fixed at the subsequential times. Having prepared the system in this way we can now perform the desired simulation.

IV. THE CROSS SECTION

We start by considering van Hove's expression for the differential scattering cross section per unit solid angle and unit interval of outgoing energy of the scattered neutron in the first Born approximation for coherent scattering:

$$\frac{d^2\sigma_{coh}}{d\Omega d\epsilon}=N\frac{a^2}{\hbar}\frac{q_f}{q_i}S(\mathbf{k},\omega), \tag{6}$$

where the dynamical structure factor[14,15] is

$$S(\mathbf{k},\omega)=\frac{1}{2\pi}\int_{-\infty}^{\infty}dt\ G(\mathbf{k},t), \tag{7}$$

and the generalized pair-correlation function[1,14] is

$$G(\mathbf{k},t)=\frac{1}{N}\sum_{l,l'}e^{-i\mathbf{k}\cdot\mathbf{x}(l)}e^{i\mathbf{k}\cdot\mathbf{x}(l')}\langle e^{[-i\mathbf{k}\cdot\mathbf{u}(l,t)]}e^{[i\mathbf{k}\cdot\mathbf{u}(l',0)]}\rangle. \tag{8}$$

In these equations $\mathbf{q}_i$ is the neutron initial momentum and $\mathbf{q}_f=\mathbf{q}_i-\mathbf{k}$ is the final momentum, $\hbar\omega$, which is equal to $(\hbar^2/2m)(q_i^2-q_f^2)$, is the energy transferred from the neutron to the crystal, a is the scattering length of the nuclei, $\mathbf{x}(l)$ is the position vector of the mean position of the lth atom. It can be written as $\mathbf{x}(l)=l_1\mathbf{a}_1+l_2\mathbf{a}_2+l_3\mathbf{a}_3$, where $\mathbf{a}_1,\mathbf{a}_2,\mathbf{a}_3$ are the basic vectors of the lattice and the l's are integers; $\mathbf{u}(l,t)$ is the time-dependent displacement of the atom away from its mean position. The angle brackets denote the thermal average. The problem of evaluating the multiphonon contribution to the cross section depends on the evaluation of the correlation function $\langle e^{[-i\mathbf{k}\cdot\mathbf{u}(l,t)]}e^{[i\mathbf{k}\cdot\mathbf{u}(l',0)]}\rangle$.

The measured spectra are related to the one-phonon cross section[1,16] given by

$$S_1(\mathbf{k},\omega)=\frac{e^{-2W}}{2\pi}\sum_{l,l'}\exp\{-i\mathbf{k}\cdot[\mathbf{x}(l)-\mathbf{x}(l')]\}\times\int_{-\infty}^{+\infty}dt\ e^{i\omega t}\langle\mathbf{k}\cdot\mathbf{u}(l,t)\mathbf{k}\cdot\mathbf{u}(l',0)\rangle, \tag{9}$$

where the Debye-Waller factor can be approximated[17] by

$$e^{-2W}=e^{-2\langle(\mathbf{k}\cdot\mathbf{u})^2\rangle}. \tag{10}$$

In this case the single phonon excited by the neutron interacts both with the harmonic and anharmonic Hamiltonian of the crystal. The width associated with the one-phonon peak is determined by the anharmonicity of the crystal. In our MD calculations the expectation value on the anharmonic crystal is replaced by a time average over the starting time τ.

The generalized pair-distribution function[4] becomes

$$G(\mathbf{k},t)=\lim_{T\to\infty}\sum_{l,l'}\exp\{-i\mathbf{k}\cdot[\mathbf{x}(l)-\mathbf{x}(l')]\}\times\frac{1}{T-t}\int_0^{T-t}d\tau e^{-i\mathbf{k}\cdot\mathbf{u}(l,t+\tau)}e^{i\mathbf{k}\cdot\mathbf{u}(l',\tau)}. \tag{11}$$

In the MD calculations we consider an fcc Al supercell with ten cubes along each of the three orthogonal axes, giving a total of 4000 particles, at $T=80$ K, and with five cubes along each direction, giving a total of 500 particles, at $T=300$ K and at $T=900$ K. Periodic boundary conditions are imposed. The time step is chosen according to the mean value of the displacement in order to properly integrate the equations of motion. $\Delta\tau$ is in the range of 10^{-14} sec. More precisely we take $\Delta\tau=0.529\times10^{-14}$ sec at $T=80$ K and $\Delta\tau=0.265\times10^{-14}$ sec at $T=300$ K and $T=900$ K. The total simulation time is of the order of a nanosecond. The $S(\mathbf{k},\omega)$ obtained in this way has been convoluted with a Gaussian resolution function[18] in order to reduce the noise in the spectrum that arises from numerical round off of errors.

The convolution is made by centering the Gaussian curve at a frequency $\bar{\omega}$ and replacing $S(\mathbf{k},\omega)$ with[18]

$$S(\mathbf{k},\bar{\omega})=\frac{1}{\sqrt{\pi}\Delta\omega}\int d\omega\ S(\mathbf{k},\omega)e^{-[\omega-\bar{\omega}]^2/\Delta\omega^2}. \tag{12}$$

At this point we study the range of temperature in which $S(\mathbf{k},\omega)$ given by Eq. (8) can be approximated by the one-phonon dynamical structure factor $S_1(\mathbf{k},\omega)$. The line shape of the dynamical structure factor and the Debye-Waller structure factor depends critically on the magnitude of the scattering momentum $\mathbf{k}=\mathbf{q}+\mathbf{G}$, where $\mathbf{q}$ is inside the first Brillouin zone (BZ) and $\mathbf{G}$ is a reciprocal lattice vector. In the experimental results the frequencies and the widths of the peaks are given as a function of $\mathbf{q}$ (Refs. 6 and 19) and not of the scattering momentum $\mathbf{k}$. To study the effect of the momentum transfer on the line shape we have performed calculations for $\mathbf{q}_{BZ}=2\pi/a\ (1\,0\,0)$ and for $\mathbf{k}=3\mathbf{q}_{BZ}$ to simulate a real experiment. The full width at half maximum of the convolution Gaussian has been chosen as a function of the

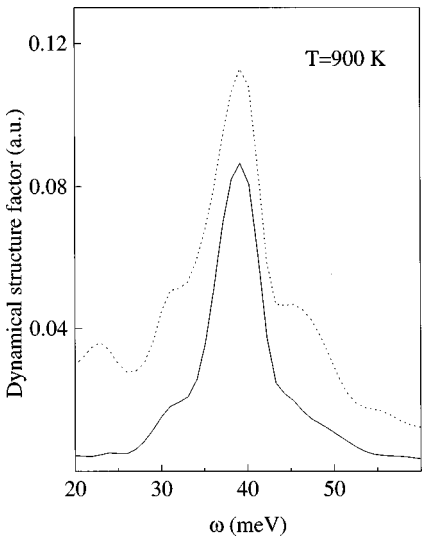

FIG. 1. Dynamical structure factor $S(\mathbf{q},\omega)$, dashed line, and one-phonon cross section $S_1(\mathbf{q},\omega)$, full line, for $\mathbf{q}=2\pi/a$ (300).

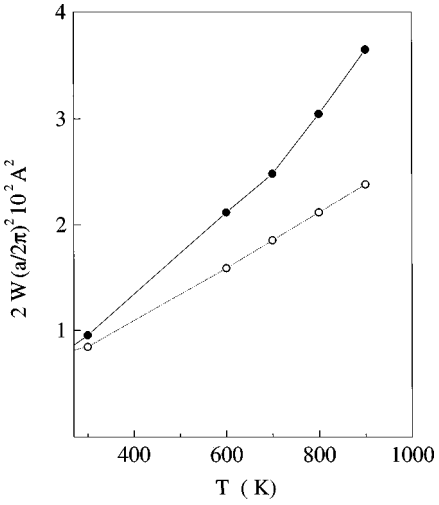

FIG. 2. The harmonic Debye-Waller factor (dashed line) compared with the one calculated with MD simulation (full line).

branch index, the reduced wave vector, and the temperature studied, in the range of 0.2–0.5 meV for $T=80$ K and of 0.4–0.7 meV for $T=300$ K.

We perform calculations at $T=80$ K, $T=300$ K, and $T=900$ K. The values of $S(\mathbf{q}_{BZ},\omega)$ and $S_1(\mathbf{q}_{BZ},\omega)$ nearly coincide for $\mathbf{k}=\mathbf{q}_{BZ}$ up to 900 K. Only for $\mathbf{k}=3\mathbf{q}_{BZ}$ at $T=900$ K the approximation starts to break down, as seen in Fig. 1. For this reason it is legitimate to use $S_1(\mathbf{q},\omega)$ to interpret the neutron data up to room temperature for $\mathbf{q}$ inside the BZ.

V. RESULTS

We consider the one-phonon pair-correlation function given[1] by

$$G_1(\mathbf{q},t)=\frac{e^{-2W}}{2\pi}\sum_{\alpha,\beta} q_\alpha q_\beta g_{\alpha\beta}(\mathbf{q},t), \tag{13}$$

with

$$g_{\alpha\beta}(\mathbf{q},t)=\lim_{T\to\infty}\frac{1}{T-t}\frac{1}{N}\sum_{l,l'}\int_0^{T-t} d\tau\, u_\alpha(l,t+\tau)u_\beta(l',t) \times e^{i\mathbf{q}\cdot[\mathbf{x}(l)-\mathbf{x}(l')]}. \tag{14}$$

The Fourier transform can be written as[16,18]

$$S_{\alpha\beta}(\mathbf{q},\omega)=\lim_{T\to\infty}\frac{1}{T}\frac{1}{N}\int_0^T dt\, u_{\mathbf{q}\alpha}(t)e^{i\omega t} \times\int_0^T dt'\, u_{-\mathbf{q}\beta}(t')e^{-i\omega t'}, \tag{15}$$

according to the Wiener-Khinchine theorem with

$$u_{\mathbf{q}\alpha}(t)=\sum_l e^{i\mathbf{q}\cdot\mathbf{x}(l)}u_\alpha(l,t). \tag{16}$$

The evaluation of $\langle u^2\rangle$ appearing in $2W$ with the MD simulation does not depend critically on the number of particles and on the length of the simulation, hence using $N=500$ particles and a simulation time of 100 psec we obtain u_l^2 independent on the cell index, as required by translational invariance with the fulfillment of $\langle u_x^2\rangle=\langle u_y^2\rangle=\langle u_z^2\rangle$. The Debye-Waller factor as a function of the temperature is drawn in Fig. 2. In our classical approach it is linear in T in the range between $T=80$ K and $T=700$ K, while at higher temperatures there is a change of slope. We have also evaluated the Debye-Waller factor in the harmonic approximation using a Debye model in the high-temperature limit.[20] The average speed of sound is evaluated from the experimental data as follows:

$$\frac{3}{v_a^3}=\sum_j\left[\frac{g(111)}{v_j(111)^3}+\frac{g(110)}{v_j(110)^3}+\frac{g(100)}{v_j(100)^3}\right] \times\frac{1}{g(111)+g(110)+g(100)}, \tag{17}$$

where the g's are the stars of $\mathbf{q}$ in the measured symmetry directions and v_j is the speed of sound in the jth branch. The Debye temperature results to be $\theta=308$ K. The harmonic Debye-Waller factor is also plotted in Fig. 2 as dashed line. Up to room temperature the two Debye-Waller factors coincide but the slope is different. The difference in the slope is due to the anharmonic part of the potential and is a measure of the importance of the multiphonon scattering events. In Fig. 2 is also present a second change of slope around 700 K. Our MD analysis explains this change of slope. In fact above 700 K the system starts to lose the fcc lattice geometry.

In Fig. 3 we present the calculation of the $g_{xx}(\mathbf{q},t)$ for $\mathbf{q}=2\pi/a$ (0.8 0 0) performed at $T=80$ K. In this case to achieve convergence in the results we have considered 4000 particles. As seen from Fig. 3(a), $G_1(\mathbf{q},t)$ cannot be approximated by an exponent of the form $e^{-\Gamma t}$. This means that the dynamical structure factor does not have a Lorentzian shape. As shown by Maradudin and Fein, $S(\mathbf{q},\omega)$ has a Lorentzian form only when cubic anharmonicity is considered in the Hamiltonian. Our results indicate the importance of the quartic and higher-order anharmonicity in the multiphonon pro-

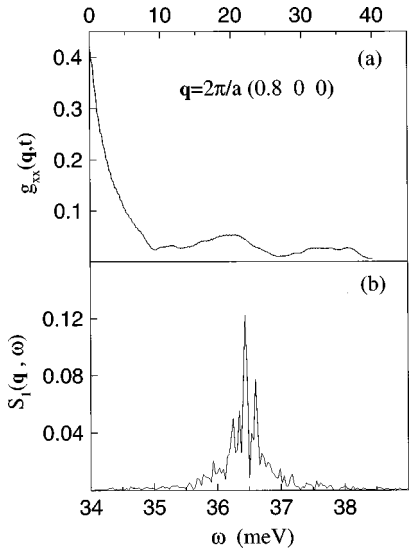

FIG. 3. (a) Correlation function at $T=80$ K. (b) Correspondent one-phonon cross section.

cesses. In Fig. 3(b) are presented the raw data of $S_1(\mathbf{q},\omega)$. The linewidth $\Gamma(\mathbf{q},\omega)$ is obtained by convoluting with Eq. (13) the raw data obtained by evaluating $S_1(\mathbf{q},\omega)$ and taking the width of the one-phonon peak at half maximum.

We compare our calculations with the extensive experimental data on Al performed by Stedman and Nilsson.[6] We start by considering phonons in the Δ direction. In Figs. 4 and 5 are depicted our calculations of the phonon widths for longitudinal phonons and transverse phonons, respectively. Panel (a) refers to $T=300$ K, while panel (b) is relative to $T=80$ K. Comparing the results for longitudinal and transverse modes it can be seen that by increasing the temperature the linewidths increase noticeably, and especially those of the transverse branch. The calculations reproduce quite well the experimental results. At $T=300$ K a well-developed peak is present around the zone boundary. The presence of this peak was explained by some of us[21] in terms of three-phonon scattering. The agreement with the full calculation is an indication of the importance of the cubic anharmonicity

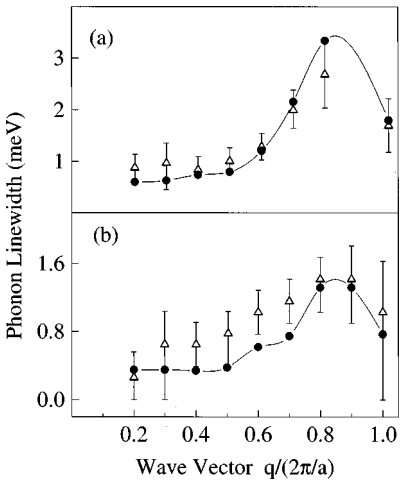

FIG. 4. (a) Linewidths for the longitudinal branch at $T=300$ K in [100] direction. Solid circles: calculated values. (b) As for (a), but for $T=80$ K.

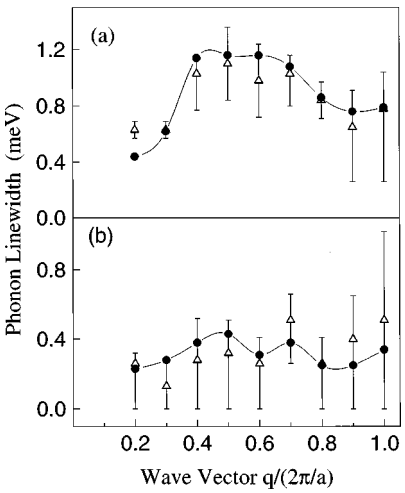

FIG. 5. As in Fig. 4, but for the transverse branch.

for this scattering geometry. In the previous work[21] the calculated linewidths with only cubic anharmonicity at small $\mathbf{q}$ were much smaller than the experimental ones. Our results indicate that at small momentum the conservation of energy and momentum can be satisfied by many processes, involving several phonons around the Γ point.

We now discuss the energy shift. Our calculations show that the position of the maximum in $S(\mathbf{q},\omega)$ is very sensitive to the number of particles. Convergent results have been obtained using $N=4000$ particles and a simulation time of 30 psec. At 80 K the MD calculations agree very well with the phonon frequencies evaluated in the harmonic approximation at $T\simeq 0$ K.[8] For this reason the energy shifts evaluated at 300 K are defined as $\Delta\omega=\omega(T=300\ \text{K})-\omega(T=80\ \text{K})$.[1] We present the energy shifts for the Δ direction in Fig. 6. Our calculations reproduce the experimental trend[7] as a function of $\mathbf{q}$ even if the error bar of the experimental data[6,22] is large. The multiphonon scattering is playing a different role for different values of $\mathbf{q}$. We do not obtain a shift proportional to ΔT as obtained in Ref. 1 by considering three- and four-phonon processes. The calculations reproduce the maxi-

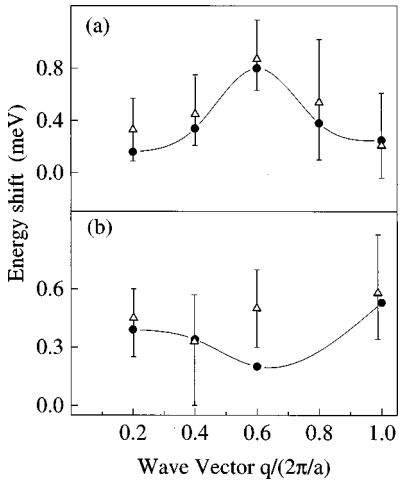

FIG. 6. (a) Energy shifts for the longitudinal branch between phonon modes at $T=80$ K and $T=300$ K in [100] direction. Solid circles: calculated values. (b) As for (a), but for the transverse branch.

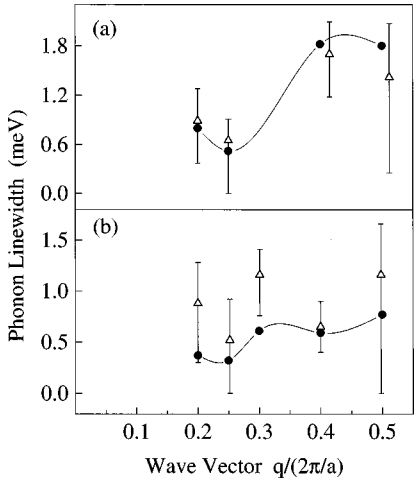

FIG. 7. (a) Linewidths for the longitudinal branch at $T=300$ K in [111] direction. Solid circles: calculated values. (b) As for (a), but for $T=80$ K.

mum present for longitudinal phonons around $\mathbf{q}=2\pi/a$ (0.5 0 0). For the transverse phonons our calculations underestimate the frequency shift at $\mathbf{q}=2\pi/a$ (0.6 0 0). However, in general, the calculations prove that the energy shifts are determined entirely by higher-order phonon interactions.

In Figs. 7 and 8 are presented the linewidths, respectively, for longitudinal and transverse phonons in the Λ direction at 300 and 80 K. Again multiphonon processes are more important for the longitudinal phonons. The linewidth of transverse phonons is much smaller than the linewidth of the longitudinal phonons. Our calculations reproduce in a satisfactory way the experimental results. The maximum around $\mathbf{q}=2\pi/a$ (0.4 0.4 0.4) at $T=300$ K can be mainly imputed according to our previous calculations to cubic anharmonicity.[21] We also note that the minimum at $\mathbf{q}\simeq 2\pi/a$ (0.25 0.25 0.25) in the direction of longitudinal phonons is practically independent on temperature. The energy shifts are depicted in Fig. 9. In this case the experimental data present an anomalous negative energy shift around the zone boundary that is also reproduced by our calculations.

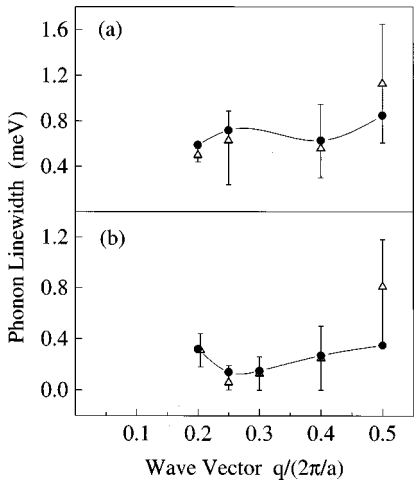

FIG. 8. As in Fig. 7, but for the transverse branch.

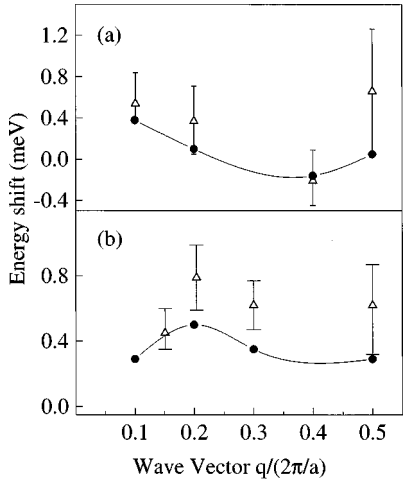

FIG. 9. (a) Energy shifts for the longitudinal branch between phonon modes at $T=80$ K and $T=300$ K in [111] direction. Solid circles: calculated values. (b) As for (a), but for the transverse branch.

In Figs. 10 and 11 we draw the linewidth in the Σ direction at 80 and 300 K. Again multiphonon scattering events favor the longitudinal modes. In this case the increase of T enhances strongly the linewidth of the longitudinal mode in the region of the small and large momentum producing a well-defined deep at $\mathbf{q}\simeq 2\pi/a$ (0.4 0.4 0) at $T=300$ K. In this direction, as shown in Fig. 12, the experimental energy shifts are in good agreement with the results of the MD simulations.

VI. CONCLUSIONS

In this paper we have shown that it is feasible to evaluate the dynamical structure factor $S(\mathbf{q},\omega)$ with a classical MD simulation. The evaluated linewidth turns out to be very sensitive to the number of particles and to the total simulation time. To reach convergence in the results, especially at small

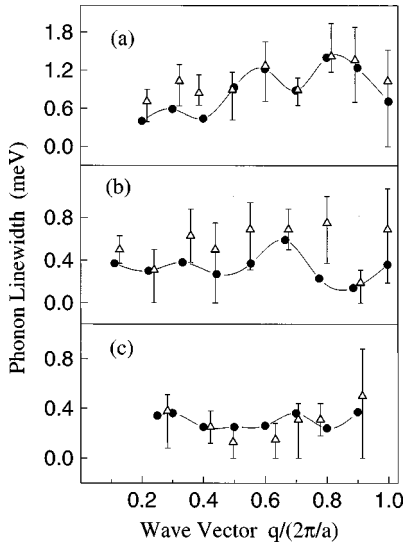

FIG. 10. (a) Linewidths for the longitudinal branch at $T=80$ K in [110] direction. Solid circles: calculated values. (b) As for (a), but for the high transverse branch $T1$. (c) As for (a), but for the low transverse branch $T2$.

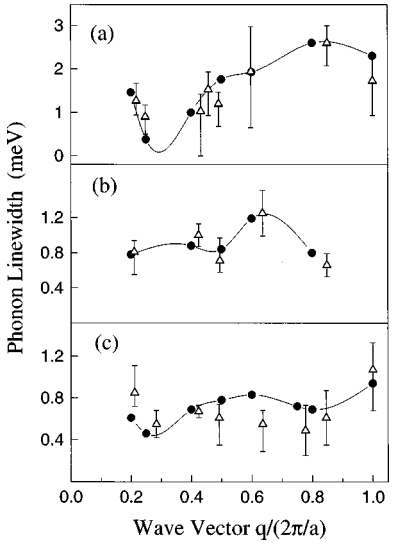

FIG. 11. As in Fig. 10, but for $T=300$ K.

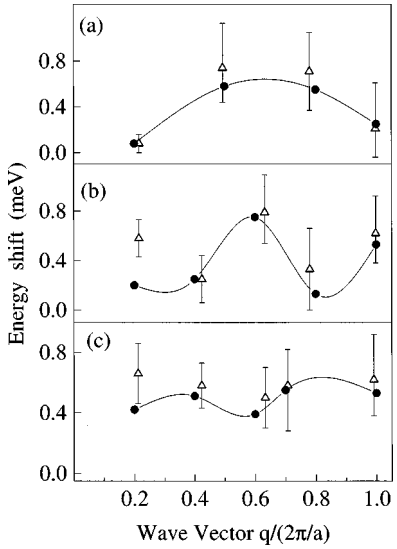

FIG. 12. (a) Energy shifts for the longitudinal branch between phonon modes at $T=80$ K and $T=300$ K in [110] direction. Solid circles: calculated values. (b) As for (a), but for the high transverse branch $T1$. (c) As for panel (a), but for the low transverse branch $T2$.

q, 4000–5000 particles and a long simulation time ($\simeq$1 nsec) are needed. For this reason the calculations have been performed with an analytical form of the potential. The many-body potential that we have used explains in a very satisfactory way the experimental data. We have also proved that for a large range of temperature the total cross section coincides with the one-phonon approximation. Close to the zone boundary the evaluated linewidths are rather close to those evaluated by considering three-phonon scattering events, while for small **q**, we prove that higher-order anharmonic interactions are essential in order to reproduce the experimental widths. The evaluated energy shift is negligible up to 80 K, so that the experimental frequencies at low temperature can be assumed as those of the harmonic crystal. The energy shift at 300 K agrees very well with the experimental values and we also reproduce the negative energy shift observed in the Λ direction.

ACKNOWLEDGMENT

One of us (G.S.) acknowledges partial financial support from NATO, Collaborative Research Grant CRG971622.

[1] A. A. Maradudin and A. E. Fein, Phys. Rev. **128**, 2589 (1962).
[2] A. A. Maradudin and V. Ambegaokar, Phys. Rev. **135**, A1071 (1964).
[3] L. van Hove, Phys. Rev. **95**, 249 (1954).
[4] R. J. Glauber, Phys. Rev. **98**, 1092 (1955).
[5] J. Kokkedee, Physica (Amsterdam) **28**, 374 (1962).
[6] R. Stedman and G. Nilsson, Phys. Rev. **145**, 492 (1966).
[7] *Numerical Data and Functional Relationships in Science and Technology*, edited by K. H. Hellwege and J. L. Olsen, Landolt-Börnstein, New Series, Group III, Vol. 13, Pt. a (Springer, Berlin, 1981), p. 11.
[8] F. Ercolessi and J. B. Adams, Europhys. Lett. **26**, 583 (1994).
[9] F. Ercolessi, E. Tosatti, and M. Parrinello, Phys. Rev. Lett. **57**, 719 (1986); Philos. Mag. A **58**, 213 (1988).
[10] M. S. Daw and M. I. Baskes, Phys. Rev. B **29**, 6443 (1984).
[11] A. Rahman, in *Correlation Functions and Quasiparticles Interactions in Condensed Matter*, Vol. 35 of *NATO Advanced Study Institute, Series B: Physics*, edited by editor (Plenum, New York, 1977).
[12] M. P. Allen and D. J. Tildesley, *Computer Simulation of Liquids* (Oxford University Press, New York, 1987).
[13] M. Parrinello and A. Rahman, J. Appl. Phys. **52**, 7182 (1981).
[14] A. Rahman, K. S. Singwi, and A. Sjölander, Phys. Rev. **100**, 756 (1955).
[15] G. Baym, Phys. Rev. **121**, 741 (1961).
[16] J. P. Hansen and M. L. Klein, Phys. Rev. B **13**, 878 (1976); J. Phys. (Paris) **35**, L-29 (1974).
[17] A. A. Maradudin, P. A. Flinn, and S. L. Ruby, Phys. Rev. **126**, 9 (1962).
[18] A. R. McGurn, A. A. Maradudin, R. F. Wallis, and A. J. C. Ladd, Phys. Rev. B **37**, 3964 (1988).
[19] B. N. Brockhouse and A. T. Stewart, Phys. Rev. **100**, 756 (1955).
[20] J. Callaway, *Quantum Theory of the Solid State*, Student ed. (Academic Press, San Diego, 1974), pp. 49 and 50.
[21] M. Zoli, G. Santoro, V. Bortolani, A. A. Maradudin, and R. F. Wallis, Phys. Rev. B **41**, 7507 (1990).
[22] T. Högberg and R. Sandström, Phys. Status Solidi **33**, 169 (1969).